

Heavy quark potential in SU(2) lattice gauge theory

John D. Stack

*Department of Physics, University of Illinois at Urbana-Champaign,
1110 West Green Street, Urbana, Illinois 61801*

(Received 7 September 1982)

Using Monte Carlo methods and the icosahedral approximation to SU(2), the heavy quark potential has been determined for SU(2) lattice gauge theory. The range of distances covered is 0.05 fm to 1 fm for a string tension of 400 MeV. The results are compared to perturbation theory, string theory, and the phenomenological potential of Martin. A simple Coulomb plus linear form gives a good overall representation of the potential.

I. INTRODUCTION

The chromodynamic potential between a heavy quark and antiquark arises from a fundamental force and as such certainly ranks in importance with the Coulomb potential between electric charges and Newton's gravitational potential between bodies with mass. Yet in contrast to its two more famous predecessors, the quark potential does not admit a simple theoretical treatment. Even with infinitely heavy sources, the calculation of the potential is highly nontrivial, due to the nonlinear dynamics of gauge fields. Computer simulations of lattice gauge theories are currently playing an important role in understanding this dynamics. This paper reports on our Monte Carlo calculations of the heavy quark potential for SU(2) lattice gauge theory without fermions. This theory is believed to have a heavy quark potential which is similar in all its features to that for lattice QCD, but is obviously simpler to treat computationally. Actually, in order to work on relatively large lattices, we simplified further and replaced SU(2) by its 120-element icosahedral subgroup \bar{I} . However, the physics remains that of SU(2), since in the region of interest to us here, Petcher and Weingarten,¹ and Bhanot and Rebbi² have previously shown that the 120-element subgroup produces results indistinguishable from full SU(2).

Our results, which build on previous calculations of the string tension K , determine the continuum heavy quark potential up to a single overall constant for SU(2) pure gauge theory, over the range $0.1 \leq x \leq 2.0$, where $x = R/\xi$, R is the interquark separation, and ξ is the correlation length which is essentially $1/\sqrt{K}$. The precise definition of ξ is given in (1) and (2) below. In the units of hadron physics, this range of separations is equivalent to $0.05 \text{ fm} \leq R \leq 1 \text{ fm}$, if \sqrt{K} is given the realistic value of 400 MeV. This is the important range of

distances for ψ and Υ spectroscopy and is also a range where analytic methods are ineffective at present, giving a strong motivation for extending the results obtained here to QCD itself.

The x values we probed in this calculation were determined by our computer resources. In any calculation on a finite lattice, there are three characteristic lengths on which a physical quantity can depend in principle; the lattice spacing a , the correlation length ξ , and the lattice size L . For the continuum limit, we want the system to have "forgotten" a and L , leaving ξ as the only relevant length. Formally, this requires $\xi/a \rightarrow \infty$ and $L/\xi \rightarrow \infty$. However, as first shown by Creutz,³ Monte Carlo calculations on a finite lattice in $d=4$ show continuum renormalization-group behavior for $\xi/a \gtrsim 2$, so the system loses its dependence on a extremely rapidly. As ξ grows, finite-lattice-size effects will eventually cause distortions in any physical quantity when ξ becomes comparable to the lattice size L . The two requirements $\xi/a \gtrsim 2$ and $\xi/L \lesssim 1$ determine a range of couplings for which continuum information can be obtained in a given calculation. The present work was done on lattices $16a \times L^3$ in size, at various L from $L=8a$ to $16a$. To determine the corresponding β values, we need a measure of ξ . The string tension K sets the physical length scale in considerations of the quark potential and it is natural to define ξ to be proportional to $1/\sqrt{K}$, with a coefficient of ~ 1 . To be specific, we define

$$\xi = 0.012/\Lambda_L, \quad (1)$$

where Λ_L is the usual two-loop expression for the Λ parameter on a Euclidean lattice,

$$\Lambda_L = (1/a)(6\pi^2\beta/11)^{51/121} \exp(-3\pi^2\beta/11). \quad (2)$$

We chose the coefficient of $1/\Lambda_L$ in (1) to be close to previous Monte Carlo estimates of Λ_L/\sqrt{K} .¹⁻⁴

Figure 1 shows the plot of ξ vs β , using (1). As can be seen from a glance at this figure, if we require that $2 \leq \xi/a \leq 16$, the present calculation can make contact with the continuum limit for the approximate interval $2.3 \lesssim \beta \lesssim 3.1$.

Allowing ξ/L to range up to ~ 1 may be overly generous. However, by studying various values of L/a from 8 to 16, we have found that distortions due to finite lattice size are less severe in SU(2) lattice gauge theory than in a typical Abelian gauge theory, where the more stringent requirement $\xi/L \lesssim \frac{1}{3}$ is reasonable.⁵ Even allowing $\xi \sim L$, Fig. 1 shows that it will be difficult with present-day computers to study the continuum limit for β significantly larger than 3.0, due to the exponential growth of ξ with β .

We deduced the quark potential from Monte Carlo data for rectangular Wilson loops, $W(T,R)$. As described in more detail in Sec. II, runs were made at a number of different β values in the interval $2.2 \leq \beta \leq 3.1$. (The values $\beta=2.2$ and 2.25 violate somewhat our criterion that ξ be at least two lattice spacings. They were included to try to gain more information on the large- R potential.) In this interval, the quark potential $V(R)$, which has had the quark self-energy removed, hopefully has negligible dependence on the lattice size and lattice spacing, so we can regard ξV as a scaling function, i.e., a function solely of $x = R/\xi$. We calculated Wilson loops only for $R/a = 1, 2, 3, 4$ so each value of β gives the potential at just four values of x . However, by varying β , we can vary x continuously, even though R/a is discrete. The number of different x values at

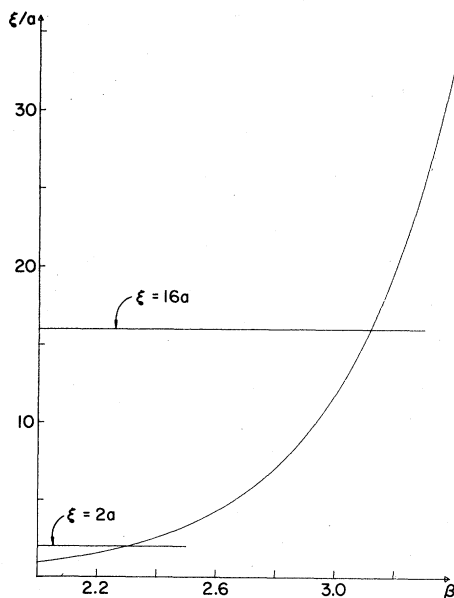


FIG. 1. ξ vs β , using (1) and (2).

which we can calculate the potential and the spacing between them is then limited only by the available computer time. The largest x values ($x_{\max} \sim 2$) come from the smallest β values, while the smallest ($x_{\min} \sim 0.1$) come from the largest β values. In this way, we can map out ξV as a function of x , in principle as accurately as desired, over the interval $x_{\min} \leq x \leq x_{\max}$. The assumption that the results do not depend on L can be tested by working on lattices of different size, and the assumption that the results are independent of the lattice spacing a can be tested by seeing how well scaling works.

Even in the scaling region, the potential deduced directly from Wilson loops is not the continuum potential $V(R)$, but rather a quantity we call the lattice potential and denote by $V_l(R)$. For T sufficiently large compared to R we have

$$W(T,R) \sim \exp[-TV_l(R)]. \quad (3)$$

The relation between the continuum and lattice potentials is

$$V_l(R) = V(R) + V_0, \quad (4)$$

where V_0 is lattice-spacing dependent and R independent, i.e., $V_0 = g(\beta)/a$, for some function $g(\beta)$. Physically, V_0 represents the self-energy of the infinitely heavy quarks which sit on the perimeter of the Wilson loop. It contributes a term proportional to the perimeter of the loop in the exponent of $W(T,R)$ and means that $W(T,R)$ is not a scaling function, but has dependence on R/a and T/a in addition to R/ξ and T/ξ . If we were using only one value of β , V_0 would be a harmless constant. But in order to merge results at different β values together and use scaling, it is essential to eliminate V_0 . Our procedure for doing this is described in detail in Sec. III. In essence, it is very simple. Since V_0 is independent of R , it does not appear in the force between two quarks. The force at a set of discrete points in x can be gotten by forming the differences $[V_l(R+a) - V_l(R)]/a$. (In practice, we use only $R=a$. See Sec. III for further discussion.) Putting a smooth curve through these points and integrating numerically, we get a determination of the continuum potential up to a constant of integration. After this arbitrary constant is chosen, a value of V_0 can be determined at each β by applying (4) at, for example, $R=a$. We can then test the self-consistency of the whole procedure. Removing $V_0(\beta)$ from the lattice potentials $V_l(R)$, multiplying by ξ , and plotting versus x should map all the Monte Carlo data onto a smooth curve which represents the continuum potential. This works quite well and is a nontrivial test, since only half the Monte Carlo data are used in the numerical integra-

tion.

In Sec. IV, we discuss various fits to the potential in both large- and small-distance regions, and using a phenomenological potential applied very success-

fully to heavy quark spectroscopy by Martin. We find that a good overall description of the potential can be obtained with a simple linear plus Coulomb fit.

II. MONTE CARLO METHOD AND WILSON LOOPS

A. Monte Carlo parameters

We used the Wilson action, namely,

$$S = \frac{\beta}{2} \sum_{\vec{k}, \vec{l}} \text{tr} [1 - U_k(\vec{x}) U_l(\vec{x} + \vec{k}a) U_k^\dagger(\vec{x} + \vec{l}a) U_l^\dagger(\vec{x})]. \quad (5)$$

The link variable $U_k(\vec{x})$ is an element of the group \bar{I} , in the representation which is the restriction to \bar{I} of the fundamental representation of SU(2). [If we refer to the SU(2) quantum number as isospin, then the first five irreducible representations of SU(2) with isospin $\frac{1}{2}$, 1, $\frac{3}{2}$, 2, and $\frac{5}{2}$ are also irreducible when restricted to \bar{I} .]

Given the action, the goal of the Monte Carlo process is to generate a sequence of configurations [sets of $U_k(\vec{x})$] with weight proportional to $\exp(-S)$. The basic step is the "link update," which begins by generating a trial link $U'_k(\vec{x})$, by multiplying the present link with a group element randomly chosen from the 12 nearest neighbors of the group identity. The decision to accept the trial link $U'_k(\vec{x})$ or retain $U_k(\vec{x})$ is then made by applying the standard Metropolis algorithm.⁶ In our calculations, the rate at which trial links were accepted varied from $\sim 40\%$ near $\beta = 2.3$ to $\sim 25\%$ near $\beta = 3.1$.

The restriction of the gauge group to \bar{I} has a number of computational advantages.² From the viewpoint of memory requirements, a link variable in \bar{I} can be represented by a 7-bit integer and 8 links can then be stored in one 60-bit computer word. In addition, the use of Boltzmann factor tables, group character and multiplication tables, plus standard Boolean operations (shift, mask, etc.), are useful in reducing execution time. By applying these techniques, plus tinkering with innermost loops, the method of indexing links, etc., we arrived at a final program in which a link update took approximately 50 μsec on a CDC Cyber 175.

A typical run consisted of $\sim 10^8$ link updates. The number of sweeps through the lattice varied, depending on lattice size. For example, at $\beta = 2.3$, where $\xi \sim 2a$, we ran 350 sweeps through a 16×8^3 lattice, updating each link 10 times. On the other hand, at $\beta = 3.1$, $\xi \sim 16a$ and it was important to run on a large lattice. Here we ran 80 sweeps through a 16^4 -lattice, updating each link five times. All of our runs began with a completely ordered configuration which had the group identity on every link of the

lattice. Periodic boundary conditions were used for three directions (those corresponding to L^3), while helical boundary conditions were used for the remaining direction which always had side $16a$. Data were taken at β values from $\beta = 2.2$ to 2.9 in steps of 0.05, as well as at the isolated values $\beta = 2.325, 3.0, 3.1$.

Wilson loops $W(T, R)$ with $T/a = 2-8$ and $R/a = 1-4$ were measured every sweep through the lattice. The time spent measuring Wilson loops varied from 10 to 20% of the total execution time. The loops measured were those oriented the "long" way on our $16a \times L^3$ lattices, where $L = 8a$ and $10a$ was used for $\beta < 2.6$ (with the exception of $\beta = 2.325$, where $L = 6a$ was used), and $L = 16a$ for $\beta \geq 2.6$. For $\beta \geq 2.6$, some runs were made with $L = 10a$ and $13a$ to check for finite-lattice-size effects, which were found to be small in all cases. In early runs, we recorded the characters of the loops, and then averaged these over all eight nontrivial irreducible representations of \bar{I} . However, the resulting numbers were ridiculously small for all but the first few representations, so in later runs we recorded only the loops averaged over isospins $\frac{1}{2}$, 1, $\frac{3}{2}$, and 2. Here, we concentrate on the fundamental representation, which determines the potential between two heavy quarks with isospin $\frac{1}{2}$. Where comparison is possible, our results for fundamental representation loops are in excellent agreement with the high-statistics results obtained for full SU(2) by Berg and Stehr.⁴

B. The lattice potential

There is no hard and fast rule for judging when the lattice is in equilibrium and configurations weighted with $\exp(-S)$ are actually being generated. The trial link acceptance rate and the geometrically small Wilson loops stabilize after only a few sweeps of the lattice. However, the larger loops, which have numerically smaller values, can take somewhat longer. We generally took a conservative approach

and omitted the first $\frac{1}{4}$ to $\frac{1}{3}$ of the run to ensure equilibrium, and computed the average of the loops over the rest of the run. For our runs of $\sim 10^8$ link updates, $\Delta W(T,R) \lesssim 0.007$, where $\Delta W(T,R)$ is the uncertainty in the loop mean value. The mean value of all measured loops is several times larger than $\Delta W(T,R)$ for $\beta > 2.45$, but as β decreases below 2.45, the mean value of loops with $R/a \geq 3$ and $T/a \geq 6$ becomes increasingly comparable to $\Delta W(T,R)$.

The lattice potential $V_l(R)$ measures the ground-state energy of the system of heavy quark, heavy antiquark, and gauge field. On a lattice infinite in the Euclidean-time direction, $V_l(R)$ is precisely defined by

$$V_l(R) = - \lim_{T \rightarrow \infty} \ln[W(R,T)]/T. \quad (6)$$

This formal limit is clearly not possible on a finite lattice. Instead we kept $T > R$, and tested for exponential behavior in T . Fortunately, in all cases, there is strong evidence for exponential behavior of $W(T,R)$ as soon as $T > R$. We got the value of the lattice potential by fitting $\ln W(T,R)$ to a straight line in T for $T > R$, the slope giving $V_l(R)$. The fit was standard least squares, with the points weighted with their inverse statistical errors. In Fig. 2, we show $\ln[W(T,R)]$ vs T for $\beta = 2.55$. The plots for other values of β look very similar, except that the statistical errors become steadily more visible as β decreases. For 2.2 and 2.25 we were only able to determine the potential for $R/a = 1$ and 2, due to the very small values of $W(T,R)$ for $R/a = 3$ and 4.

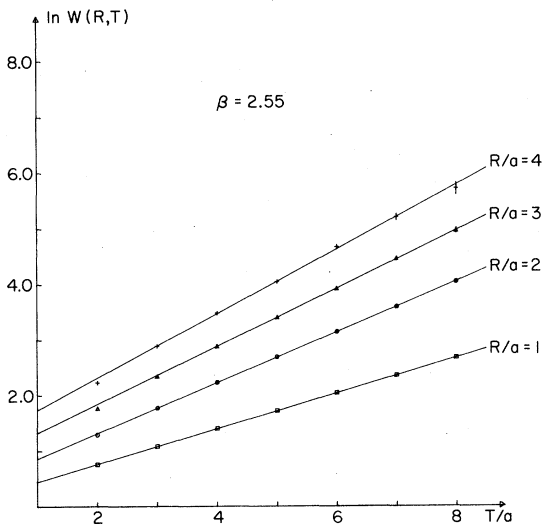


FIG. 2. $\ln W(T,R)$ vs T , at $\beta = 2.55$.

III. THE FORCE AND CONTINUUM POTENTIAL

As mentioned in the Introduction, the lattice potential does not scale, since it contains the self-energy $V_0(\beta)$. This is illustrated in Fig. 3, where we plot the dimensionless lattice potential ξV_l vs x .⁷ Our goal is to get a relative determination of $V_0(\beta)$, so that removing it from $V_l(R)$ will move the sets of points which lie on different curves in Fig. 3 onto a single curve which then will determine the continuum potential.

Since $V_0(\beta)$ is independent of R , it does not affect the force between two quarks,

$$F(R) = \frac{\partial V}{\partial R} = \frac{\partial V_l}{\partial R}. \quad (7)$$

The approach we took was to eliminate $V_0(\beta)$ by integrating the force between two quarks with respect to x . Our values for $V_l(R)$ at $R/a = 1, 2$ are statistically very accurate for all measured values of β , so these values of R/a were used to determine F . The two values $R/a = 1, 2$ define x values $x_2 = 2a/\xi$, $x_1 = a/\xi$, and their difference $\Delta x = x_2 - x_1$ at each β . In terms of these quantities, we may write the dimensionless force $\xi^2 F$ as

$$\xi^2 F(x_i) = \xi [V(x_2) - V(x_1)] / \Delta x, \quad (8)$$

where x_i lies between x_1 and x_2 and will be specified

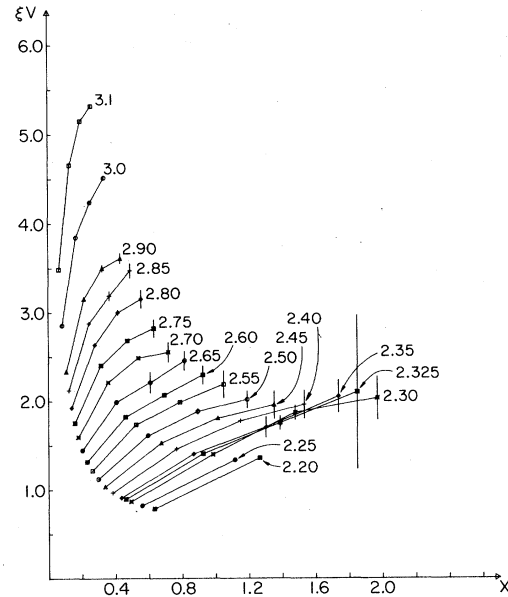


FIG. 3. The dimensionless lattice potential $\xi V_l(x)$ vs x . The same symbol represents a given β value in all succeeding plots. The solid lines connect points with the same β .

shortly. Before doing that, it is important to discuss one feature of definition (8), namely, that it tacitly assumes that the continuum limit applies at the small distances $R/a = 1, 2$. This cannot literally be true; for the system to “forget” the lattice spacing, it is necessary to be in the regime $R/a \gg 1$, R/ξ arbitrary. However, it is part of the lore of spin systems that once ξ is in the scaling region, spin-spin correlation functions assume their scaling forms quite accurately for small values of R/a , even $R/a = 1, 2$.^{8,9} (Here R refers to the distance between spins.) Since Wilson loops are the analog for lattice gauge theories of spin-spin correlation functions for spin systems, it is very natural to apply a similar assumption here, with the expectation that it will introduce some small errors ($\sim 5\%$).

Although $R/a \gg 1$ is clearly inaccessible in our calculations, it might be objected that using $R/a = 2, 3$ or $R/a = 3, 4$ to determine the force would at least be a step in the right direction. We have checked that it makes a quantitatively negligible difference to use $R/a = 2, 3$ rather than $R/a = 1, 2$ to determine $\xi^2 F$. On the other hand, using $R/a = 3, 4$ suffers from the difficulty that the statistical accuracy of $V_l(R)$ at $R/a = 4$ decreases rapidly as β falls below 2.45. Thus using $R/a = 1, 2$ seems to us to be the best procedure.

Now, let us turn to the assignment of the intermediate distance x_i . Since V_0 has dropped out of (8), the right-hand side of this equation is the difference of the dimensionless continuum potential $\xi V(x)$ at the points x_1 and x_2 , divided by their separation Δx . (There is a small penalty to be paid for violating the condition $R/a \gg 1$, as discussed above.) From (7), $\xi^2 F(x_i)$ is $\xi(\partial V/\partial x)(x_i)$. If we were really able to take the limit $\Delta x \rightarrow 0$, then x_i could be any point in the interval $[x_1, x_2]$. However, Δx is finite, ranging from 0.06 near $\beta = 3$ to 0.5 near $\beta = 2.2$. Nevertheless, the mean-value theorem of elementary calculus still states that for some x_i in the interval $[x_1, x_2]$, the right side of (8) gives the exact value of $\xi^2 F$. To get a definite result for x_i , we make the assumption that the potential can locally be represented as a linear term plus a Coulomb term, i.e., $\xi V(x) = Ax - B/x$, where A and B are either constants or functions which vary slowly compared to x and $1/x$. As discussed further in the next section, this general sort of form for the potential represents the leading behavior in both large- and small-distance regions. In between, analytic methods say nothing, but it is reasonable to apply it there also, since we expect the potential to be a smooth, simple function despite the difficulty of calculating it.

Under the assumption that A and B are either constants or slowly varying compared to x and $1/x$,

the right-hand side of (8) becomes $A + B/2(x_1)^2$. But this is the same as the derivative $\xi \partial V/\partial x$ (again ignoring the variation of A and B over the interval Δx), evaluated at $x_i = \sqrt{2}x_1$. This then fixes x_i . In Fig. 4, we show $\xi^2 F$ as determined by (8) vs x .

The next step is to numerically integrate $\xi^2 F$ to get ξV . This was done by putting a smooth curve through the points in Fig. 4, using a cubic spline interpolation. Cubic splines are widely used in interpolation and have the desirable properties of introducing minimal extraneous curvature and converging to the interpolated function as the separation between points goes to zero.¹⁰ From our point of view, using interpolation here rather than some form of least-squares fit allows us to determine V_0 locally in β and does not require a commitment on the overall shape of the potential. The interval over which the interpolation is carried out ranges from $x = \sqrt{2}a/\xi(3.1) = 0.092$ to $x = \sqrt{2}a/\xi(2.2) = 0.895$.

Once the spline interpolation to $\xi^2 F$ is made, we numerically integrate, fixing the constant of integration by assigning ξV the arbitrary value -2.0 , at $x = \sqrt{2}a/\xi(3.1)$. We can then determine the (relative) self-energy at each β by computing the difference between ξV_l and ξV as found by numerical integration. This difference is computed at the x value which corresponds to $R/a = 1$ for all β values for which this point falls in the spline interpolation interval, $R/a = 2$ otherwise. Having in this way determined a V_0 for each β , we can now move the lattice potentials of Fig. 3 relative to each other to

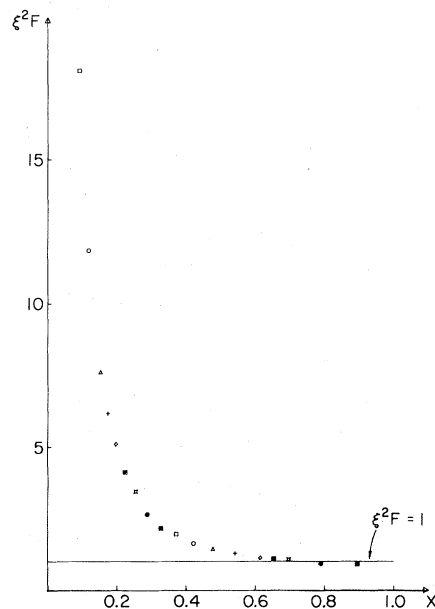


FIG. 4. The dimensionless force $\xi^2 F$ vs x .

get values which represent the continuum potential. If our procedure is self-consistent, the $R/a=3,4$ points which have not been used so far, should fall on the same curve as the $R/a=1,2$ points. The result is shown in Fig. 5. Although there are some minor violations, the overall quality of the scaling appears to be excellent.

We close this section by briefly discussing the assumptions underlying our results so far. To restate them, we have made the following assumptions. (i) The correlation length is given by (1) and (2). (ii) In the scaling region, there is only a small error introduced by working at $R/a=1,2$ rather than $R/a \gg 1$. (iii) The intermediate distance x_i is given by $x_i = \sqrt{2}x_1$, or equivalently, the potential is locally linear plus Coulomb. Note that no free, adjustable parameters have been introduced. With regard to assumption (i), it is the functional form of Eq. (2) which is important, the value for the coefficient of $1/\Lambda_L$ in (1) has been chosen merely for convenience. We have done some rough tests of this functional form by varying the exponent in (2) away from $3\pi^2/11$. The results do not scale as well as those in Fig. 4, although it would be hard to show convincingly that $3\pi^2/11$ was the correct value with our data alone. The same holds true for the $(\beta)^{51/121}$ term multiplying $\exp(-3\pi^2\beta/11)$. The form of ξ is definitely a hypothesis here from which we hope to learn about V . We have also checked assumption (iii) by varying x_i/x_1 away from $\sqrt{2}$. Here only minor variations wreck scaling, and although we have not tried to do it, our data could probably be

used to show that in order for ξV to scale, x_i/x_1 must take a value near $\sqrt{2}$. Other than the fact that the results scale well, we have no way to directly check assumption (ii).

IV. FITS TO THE POTENTIAL

A. Theory

Before discussing the various fits we have made to our Monte Carlo potential, let us review what is known theoretically, where there is understanding only in the extreme large- and small-distance regions. For $\sqrt{K}R \gg 1$, the potential is predicted¹¹ to take the limiting form

$$V(R) \rightarrow KR - \pi/12R, \quad (9)$$

where the first term is the energy of the static chromoelectric flux tube connecting the heavy quarks, and the second term arises from the fluctuations of this flux tube or string. The $1/R$ term in (9) has not yet been derived from gauge field theory, but follows from a treatment analogous to a particle path-integral description of a propagator in field theory.¹² In the analogy, K plays the same role in the string case that the mass does in the particle case. Since a particle path integral does give the correct large-distance behavior of a massive field-theory propagator, it seems quite likely that (9) is correct. The analogy would suggest that there are further correction terms to (9), involving higher inverse powers of R , but nothing is known about this at present.

At short distances, $\sqrt{K}R \ll 1$, renormalized perturbation theory makes a precise prediction for the leading behavior;

$$V(R) \rightarrow \frac{-(9\pi/22)}{RL(R)} \left[1 - \frac{102}{121} \frac{\ln[L(R)]}{L(R)} \right], \quad (10)$$

where $L(R) = 2 \ln(1/\Lambda'R)$. Correction terms to (10) can be of two types; (i) perturbative corrections (three loops and beyond), in which the basic structure remains a Coulomb term, modulated by logarithms and (ii) nonperturbative corrections, e.g., a term $\Lambda'R$, with modulating logarithms. The latter sort of corrections would be analogous to higher twist terms in electroproduction. It should be noted that if as assumed by some authors,^{13,14} the small- R behavior of $V(R)$ is controlled by the vacuum matrix elements of local operators, then the leading nonperturbative correction to ξV is of the form $(\Lambda'R)^3$, rather than $\Lambda'R$. This difference would have a negligible effect on the values of ξV at small x which were determined in the last section. The reason is that the Coulomb term dominates at small x , and therefore the value $x_i/x_1 = \sqrt{2}$ which we used is still quite accurate.

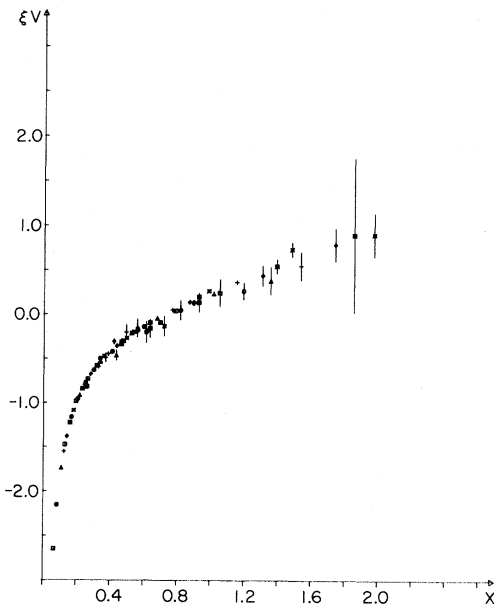


FIG. 5. The dimensionless potential $\xi V(x)$ vs x .

As has been discussed extensively in the literature, Λ parameters, although renormalization-group invariants, are not fundamental physical quantities like K , since they depend on the method of renormalization. Equation (10) is written in a scheme, natural in discussing the potential, in which there is no $[L(R)]^{-2}$ term on the right side of (10). The Λ parameter in this scheme, denoted by Λ' , is close in magnitude to $\Lambda_{\overline{\text{MS}}}$ and Λ_{MOM} and is related to Λ_L in SU(2) pure gauge theory by $\Lambda' = 56.49\Lambda_L$.^{15,16}

B. Fits to the potential

We have made a number of least-squares fits to the data for ξV determined in the last section. Most of them are motivated by our basic picture of the potential, that it can be represented locally by a Coulomb term plus a linear term. All are simple, involving at most two parameters. An attempt has been made to explore fairly thoroughly the effects of various cuts on the data; in x , the couplings included, the R/a values included, etc. Our linear plus Coulomb fits are parametrized in terms of constants $K'\xi^2$ and α as follows:

$$\xi V = (K'\xi^2)x - \alpha/x, \quad (11)$$

where ξ is always given by (1), and we will quote either $K'\xi^2$ or Λ_L/\sqrt{K} , along with α . (In the last section, $K'\xi^2$ and α were denoted as A and B .) The prime on K denotes the fact that unless the fit is restricted to large x , the linear term only determines an effective string tension. The prime on K will be dropped when discussing the large- x region of the data. Since it is extremely difficult to gather accurate Monte Carlo data for appreciable values of x , we will be very generous in deciding what constitutes a “large” value of x .

We begin by approaching the data from the perspective of large-distance physics. The main standard of comparison here is the previous Monte Carlo calculations of the string tension.¹⁻⁴ All of these calculations use the method introduced by Creutz,³ in which the string tension is extracted from ratios of nearly square Wilson loops. The basic assumption of the method is that, apart from a perimeter term, the Wilson loops obey an area law. The analogous assumption for us is that the potential is purely linear. In Fig. 6, we show the linear fit to all the data with $x \geq x_{\min} = 0.5$. The value of $K\xi^2$ is 0.94, and varies only slightly when we perform cuts such as eliminating the points with $\beta = 2.2$ and 2.25, which lie at the edge of the scaling region. However, fits of this type are not stable under an increase of x_{\min} . The value of $K\xi^2$ steadily decreases, reaching 0.83 for a linear fit to all the data with $x \geq 0.9$. Beyond $x_{\min} = 0.9$, we gradually run out of accurate

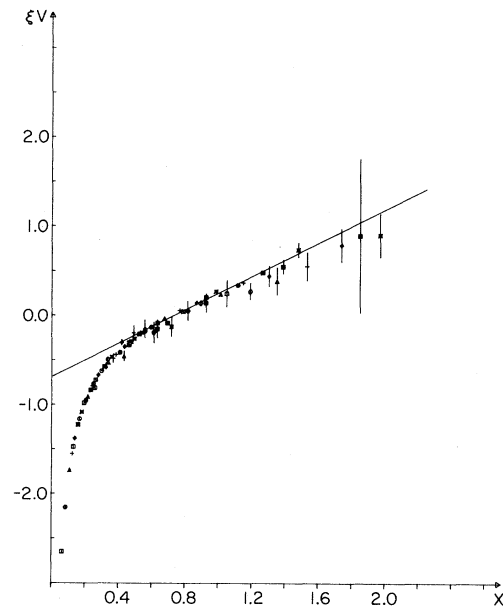


FIG. 6. Straight-line fit to ξV for $x \geq 0.5$.

data points, so the parameters for fits with $x_{\min} > 0.9$ are not very well determined. A value of $K\xi^2 = 0.83$ corresponds, using (1), to $\Lambda_L/\sqrt{K} = 0.13$, which is consistent with results obtained using Creutz ratios.¹⁻⁴

The fits just described do not really constitute an objective measure of K , since the value of $K\xi^2$ obtained was not stable. The fact that $K\xi^2$ was decreasing with increasing x_{\min} suggests the presence of an attractive Coulomb term, in addition to the linear term. We have explored the possibility of a Coulomb term for $x \geq 0.5$ in two different fits. The first constrains $\alpha = \pi/12$ as in (9). The resulting fit to all data with $x \geq 0.5$ is shown in Fig. 7. The statistical quality of this fit is about the same as the purely linear fit of Fig. 6. The value of $K\xi^2$ is now 0.50, considerably smaller than for the purely linear case. As we increase x_{\min} , we again find that the results change, but this time $K\xi^2$ increases, reaching 0.57 for $x_{\min} = 0.90$. Although the behavior of the purely linear fit suggested the presence of a Coulomb term, the value $\alpha = \pi/12$ is clearly too large, and the correct value of α apparently lies between 0 and $\pi/12$. This is confirmed by a two-parameter fit to the large- x region, where we get a best value for $K\xi^2$ of 0.72, corresponding to $\Lambda_L/\sqrt{K} = 0.014$, while $\alpha = 0.11$, less than half $\pi/12$. The errors are fairly large, $\sim 15\%$ for Λ_L/\sqrt{K} , $\sim 20\%$ for α . Thus we favor a string tension somewhat smaller than that determined with Creutz ratios. This is not surprising, since as mentioned earlier, the Creutz ratio method implicitly as-

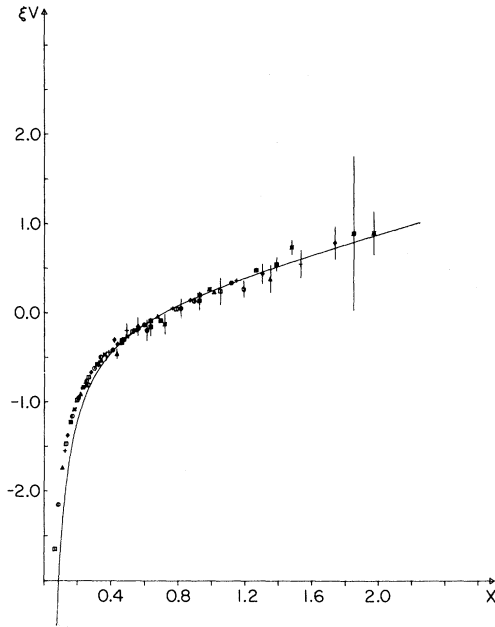


FIG. 7. Fit to ξV with $\alpha = \pi/12$, $x \geq 0.5$.

sumes a linear potential, whereas we claim that a Coulomb term is also present. The Coulomb term accounts for a small ($\sim 10\%$ at $x=1$), but measurable amount of the variation of the potential over the range of x values we are probing. Since we are not yet in the region $\sqrt{KR} \gg 1$, there is no direct conflict with the prediction (9) for α .

We now turn attention to the small- x region. The obvious first question is whether perturbation theory applies. In Fig. 8, we show two-loop perturbation theory from (10), plotted versus our data. A constant has been adjusted so that (10) goes through $x=0.065$ which is the smallest x data point. While there is brief contact between the data and perturbation theory, the data soon rise sharply above perturbation theory. As is clear from Fig. 8, perturbation theory eventually breaks down completely, but its quantitative validity probably disappears much sooner. From (10), the effective Coulomb term of two-loop perturbation theory has $\alpha=0.155$ at our smallest x value. The one-loop approximation is approximately 25% larger. There are of course no positive powers of x in straight perturbation theory.

To gain further insight into the small- x region, we performed local two-parameter fits to the data using a Coulomb term plus a linear term over intervals x_{\min} to $x_{\min} + 0.20$, with $x_{\min} = 0.0, 0.10, 0.20, 0.30$, and 0.40 . In this way, we can determine an effective local value of $K'\xi^2$ and α . The results are shown in Table I. There are several features worth noting. The value of α generally decreases as smaller x

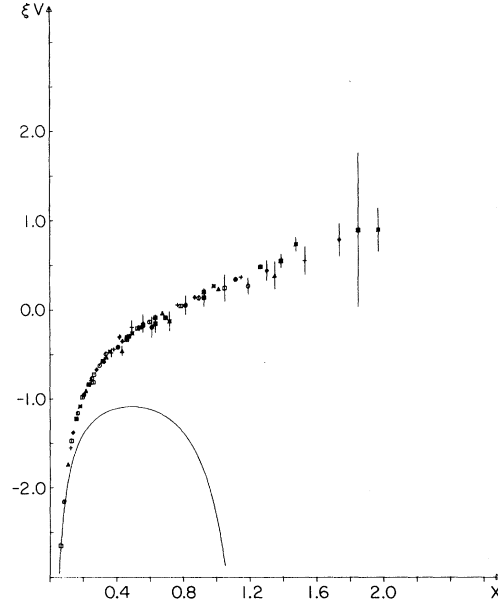


FIG. 8. Two-loop perturbation theory compared to ξV .

values are sampled. This is in qualitative accord with asymptotic freedom. Quantitatively, α is smaller than the value obtained from (10), but this is only a 10% effect at $x=0.065$ and could easily be accounted for there by higher orders in perturbation theory. It should also be remembered that although the Monte Carlo calculation is nonperturbative, in the short-distance region it is also approximate in that we are working on lattices with $\xi \sim L$ and using the icosahedral approximation to SU(2) which must eventually break down at short distances. Finally, from Table I there is clear evidence for a linear term at all the small- x values we can study. A large value of $K'\xi^2$ is found in the interval $x=0.0$ to $x=0.2$, but after that $K'\xi^2$ settles down to values of the same order of magnitude that we find at large x .

We have also studied fits using a form of the potential applied very successfully to ψ and γ spectroscopy by Martin.¹⁷ Here the potential is parametrized by

$$\xi V = A + Bx^\gamma. \quad (12)$$

TABLE I. Effective Coulomb and linear terms at short distance.

α	$K'\xi^2$	x_{\min}	x_{\max}
0.135	2.132	0.0	0.2
0.158	0.962	0.1	0.3
0.176	0.700	0.2	0.4
0.170	0.635	0.3	0.5
0.180	0.674	0.4	0.6

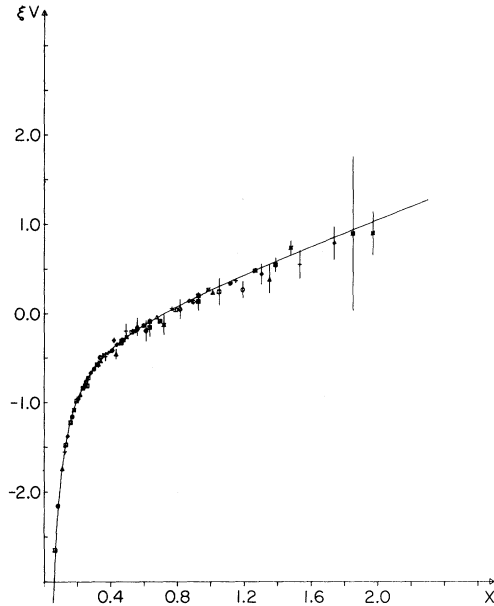


FIG. 9. Linear+Coulomb fit to all the data.

These fits do not work as well as our linear plus Coulomb fits. Further, the value of γ is very sensitive to the x interval chosen. To give three examples, a fit over the interval $x=0.15$ to $x=0.8$ gives $\gamma=-0.43$, the interval $x=0.3$ to 1.4 gives $\gamma=0.07$, while $x \geq 0.5$ gives $\gamma=0.25$.

Finally, although the effective strengths of linear and Coulomb terms both vary with x , a simple linear plus Coulomb fit to all the data actually works quite well as shown in Fig. 9. The parameters of the fit are well determined; $K'\xi^2=0.71 \pm 0.02$ and

$\alpha=0.164 \pm 0.008$. This fit is very stable against various cuts, and if there were a hadron spectroscopy for SU(2) pure gauge theory, would represent the best simple parametrization of the potential to use.

V. Conclusion

Using standard Monte Carlo methods and strong but reasonable assumptions on scaling, we have shown that the spin-independent part of the heavy quark potential can be determined for non-Abelian lattice gauge theory. Two extensions of the present work are needed in order to confront directly the rich spectroscopy of heavy quark mesons; the inclusion of spin-dependent terms in the potential and the extension to SU(3) as the gauge group. Both appear to be feasible with present-day computers, although it will clearly be necessary to work on smaller lattices than those used here for the case of an SU(3) gauge group. This may not be a difficulty, since we found that finite-lattice-size effects were small for SU(2), and recent work has suggested that they become completely negligible for SU(N) as $N \rightarrow \infty$.¹⁸⁻²⁰ Thus lattices considerably smaller than 16^4 may suffice for SU(3). We hope to report on the spin-dependent part of the potential and the extension to SU(3) in future work.

ACKNOWLEDGMENTS

I would like to thank John Kogut for discussions and help with some of the calculations, and the University of Illinois Research Board for a grant of computer time. This research was supported by the U. S. National Science Foundation, Grant No. NSF-PHY-81-09494.

¹D. Petcher and D. H. Weingarten, Phys. Rev. D **22**, 2465 (1980).

²G. Bhanot and C. Rebbi, Nucl. Phys. **B180**, 469 (1981).

³M. Creutz, Phys. Rev. Lett. **45**, 313 (1980); Phys. Rev. D **21**, 2308 (1980).

⁴B. Berg and J. Stehr, Z. Phys. C **2**, 349 (1981).

⁵G. Jongeward and J. Stack (unpublished).

⁶N. Metropolis, A. W. Rosenbluth, M. N. Rosenbluth, A. H. Teller, and E. Teller, J. Chem. Phys. **21**, 1087 (1953).

⁷The error bars shown in Fig. 3 are naive statistical errors, multiplied by 2. The values of Wilson loops are correlated from sweep to sweep, so treating them as independent tends to underestimate statistical errors. See Berg and Stehr, Ref. 4, for further discussion.

⁸M. E. Fisher and R. J. Burford, Phys. Rev. **156**, 583 (1967).

⁹M. Ferer, M. A. Moore, and M. Wortiz, Phys. Rev. Lett. **22**, 1382 (1969).

¹⁰See, for example, J. Stoer and R. Bulirsch, *Introduction to Numerical Analysis* (Springer, New York, 1980), pp. 93-106.

¹¹M. Lüscher, K. Symanzik, and P. Weisz, Nucl. Phys. **B173**, 365 (1980).

¹²J. Stack and M. Stone, Phys. Lett. **100B**, 476 (1981).

¹³C. A. Flory, Phys. Lett. **101B**, 98 (1981).

¹⁴A. Soni and M. D. Tran, Phys. Lett. **109B**, 393 (1982).

¹⁵A. Billoire, Phys. Lett. **104B**, 472 (1981).

¹⁶E. Kovacs, Phys. Rev. D **25**, 3312 (1982).

¹⁷A. Martin, Phys. Lett. **100B**, 511 (1981); **93B**, 338 (1980).

¹⁸T. Eguchi and H. Kawai, Phys. Rev. Lett. **48**, 1063 (1982).

¹⁹G. Bhanot, U. Heller, and H. Neuberger, Phys. Lett. **113B**, 47 (1982).

²⁰D. Gross and Y. Kitazawa, Princeton report, 1982 (unpublished).